Bull. Inst. Chem. Res., Kyoto Univ., Vol. 63, No. 4, 1985

Some Remarks on Imogolite Mesophase

Kanji KAJIWARA*, Nobuo DONKAI**, Yoshinori FUJIYOSHI***,
Yuzuru HIRAKI****, Hiroshi URAKAWA*****,
Hiroshi INAGAKI**

Received November 2, 1985

Imogolite, a natural product in the clay fraction of Japanese soil, was characterized through its dilute solution properties as a rigid rod in a preceding report. Succeeding this conclusion, imogolite was further characterized to evaluate its exact molecular dimension. Its cross-sectional radius of gyration was estimated from the Guinier plot for cross-section to be 10.5 A where the small-angle X-ray scattering (SAXS) data was obtained with SAXES (a focusing optics for a synchrotron at Photon Factory, Tsukuba).

We propose the acidic aqueous solution of imogolite as an ideal lyotropic system. Imogolite, though achiral, formed cholesteric spherulites in the anisotropic phase, and no temperature dependence was marked on two critical concentrations (A and B points) as predicted by the theories of Flory and Onsager. A satisfactory quantitative agreement was observed with Onsager's theory. An electron microscope revealed the raft-like imogolite sheet floating in the anisotropic phase.

KEY WORDS: Imogolite/ Guinier plot for cross section/ Lyotropic system/ Cholesteric mesophase/ A point/ B point

INTRODUCTION

A rigid rodlike molecule attracts much interest recently because of its characteristics of liquid crystal forming. Here a lyotropic mesophase formation is driven by a hard core repulsive interaction (excluded volume effect) among dense configurations of rodlike molecules[1] at sufficiently high temperatures (i.e., in the athermal limit). According to Flory[2] or Onsager,[3] the coexistence curves in the T-v_2 phase diagram form a narrow corridor in the range of two critical concentrations v_2^* (A point) and v_2^{**} (B point) where T and v_2 denote the temperature and the volume fraction of solute, respectively. v_2^* and v_2^{**} are equivalent to the limiting compositions of the pure isotropic and anisotropic phases, respectively. Completely rigid rods in isotropic solvent represent an ideal limiting case, and the critical concentrations are predicted in terms of the axial ratio x by Flory on the basis of the lattice model[2] as

$$v_2^* \sim 7.89/x \text{ and } v_2^{**} \sim 11.57/x \qquad (1a)$$

* 梶原莞爾 : Laboratory of Molecular Design for Physiological Functions, Institute for Chemical Research, Kyoto University, Uji, Kyoto 611.
** 呑海信雄, 稲垣 博 : Laboratory of Polymer Separation and Characterization, Institute for Chemical Research, Kyoto University, Uji, Kyoto 611.
*** 藤吉好則 : Laboratory of Crystal and Powder Chemistry, Institute for Chemical Research, Kyoto University, Uji, Kyoto 611.
**** 柊 弓弦 : Laboratory of Physical Chemistry of Enzyme, Institute for Chemical Research, Kyoto University, Uji, Kyoto 611.
***** 浦川 宏 : Laboratory of Fiber Chemistry, Institute for Chemical Research, Kyoto University, Uji, Kyoto 611.

or by Onsager with the virial expansion method[3] as

$$v_2^* \sim 3.29/x \text{ and } v_2^{**} \sim 4.22/x \tag{1b}$$

where the axial ratio x is defined as

$$x = L/d \tag{2}$$

with L and d being the length and diameter of a rod, respectively. Onsager's result is expected to be asymptotically exact in the limit of low concentration and large axial ratio, while Eq. (1a) is based on the lattice model and only qualitatively correct at high solute concentrations. Eqs. (1a) and (1b) are so formulated as to take into account the asymmetric repulsion only without attractive interactions, and the narrow corridor in the theoretical T-v_2 phase diagram runs parallel to the ordinate axis. The bent of the narrow corridor was, however, observed toward high concentrations as the temperature is increased in the lyotropic systems such as poly (γ-benzyl L-glutamate) (PBLG) in dimethylformamide[4] and cellulose acetate in trifluoroacetic acid.[5] As, for example, these thermotropic behavior are attributed to the temperature dependence of chain rigidity, various factors are considered as possible causes for the deviation from Flory's theory.[1] The anisotropic attractive interactions of rigid rods also cause thermotropicy in lyotropic systems.[6] A lack of an ideal system to examine the available theories quantitatively, leads to an unsatisfactory discussion on the results and leaves ambiguity to decide the fundamental factors governing the thermodynamic behavior of the system which forms liquid crystal.

Here we introduce imogolite in acetic acid aqueous solution as an ideal lyotropic system, and present some evidence that imogolite forms cholesteric liquid crystal. The analysis of the mesophase is not yet complete, but it is hoped that a present report suffices to provide basic characteristics of imogolite liquid crystals.

PREPARATION OF IMOGOLITE SOLUTIONS

Imogolite, composed of hydrated aluminium silicate, is a natural product in the clay fraction of Japanese soil from glassy volcanic ash or in weathered pumice beds. Imogolite has a characteristic geometrical profile in the bundles of linear tubes of approximately 20 A in diameter and several thausands A in length each as sketched in Fig. 1. In a preceding report,[7] we have concluded that imogolite is represented by a rigid thin rod and proposed the C_{24h} symmetry for an imogolite unit from the analysis of its dilute solution properties. That is, twelve gibbsite units form the cylinder of an imogolite unit which is 23 A and 8.4 A in diameter and length, respectively. Here the chemical composition of a gibbsite structural unit is given as $SiO_2 \cdot Al_2O_3 \cdot 2H_2O$, so that the molecular weight of an imogolite unit is equal to 4754.

Imogolite sample solutions were prepared as follows: Imogolite gel films, filling the interspaces among weathered pumice grains, were collected from a pumice bed at Murasakino (Kitakami-shi, Iwate-ken, Japan), treated with $Na_2S_2O_4$-$NaHCO_3$-$Na_3C_6H_5O_7 \cdot 2H_2O$ at 80°C and then with Na_2CO_3 to remove oxides and amorphous silicates, and washed with 30% H_2O_2 at 80°C and rinsed to eliminate organic impurities. Colorless imogolite gel thus obtained was washed further in a soxhlet ex-

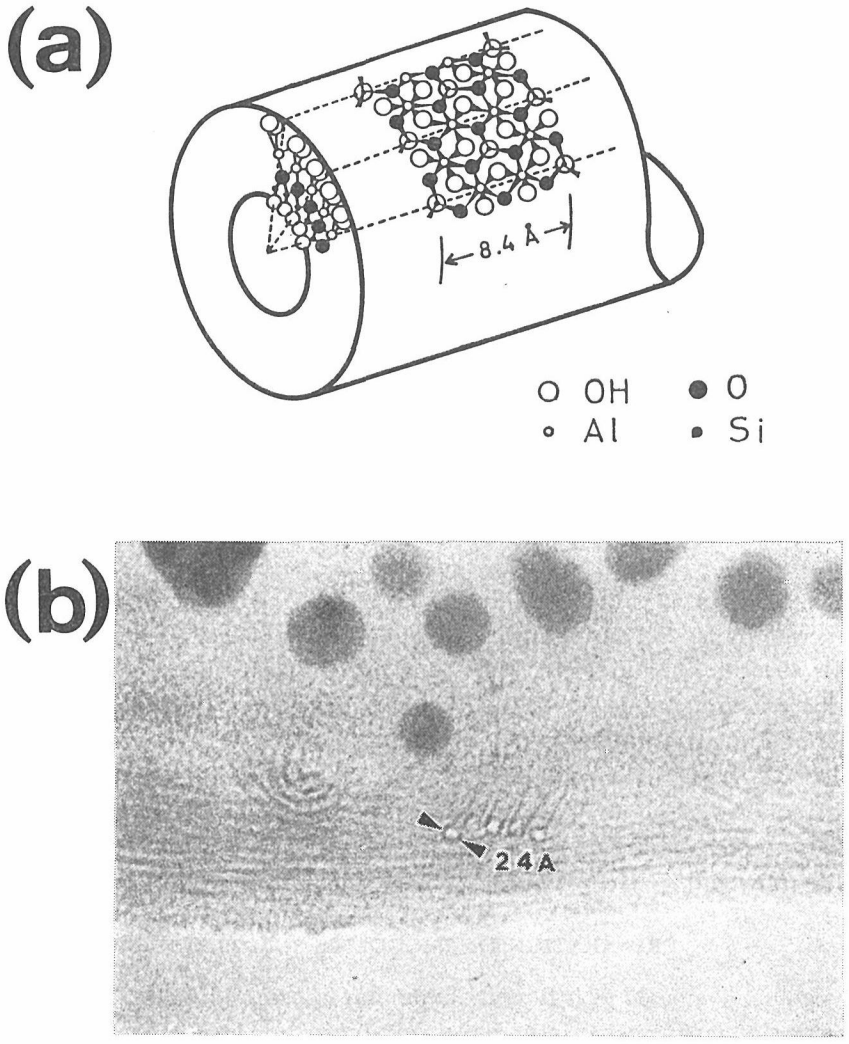

Fig. 1. A schematic view (a) and electron micrograph (b) of imogolite. A gibbsite unit is marked by dotted line.

tractor with hot aqueous solution of acetic acid of 0.03 vol% (pH 3.5) for further 3 days. Imogolite gel was dispersed in acidic aqueous solution of pH 3.0 by applying 20 KHz ultrasonic wave for a period determined previously.[7] Undissolved portions of the samples were separated by centrifugation at 10,000 *rpm* for one hour, and the supernatants were concentrated to a desired concentration in cellulose tube (Visking Co., Chicago, U.S.A.) while dialyzing against sufficient amount of aqueous solution containing 1.20 vol.% acetic acid and 0.02 wt.% NaN_3 (sterilizer). The solutions of various concentrations were then sealed in ampules and left still for at least 10 days at constant temperature to observe the phase separation.

INTRINSIC PROPERTIES OF IMOGOLITE

Imogolite possesses positive charges in an acidic solution and begins to flocculate as the pH value exceeds 7 to 7.6.[8] The strong affinity of its surface OH groups to protons develops positive charges in response to low pH values, and stabilizes imogolite solutions. Thus pH 3 was chosen to ensure molecular dispersion of imogolite in solution according to the preceding results[7] where the intrinsic viscosity $[\eta]$ is rather small and independent of pH values. Here $[\eta]$ follows an equation:

$$[\eta]=(9.35\times10^{-12})M_w^2/\ln M_w \qquad (3)$$

with M_w being the weight-average molecular weight of imogolite. The intrinsic viscosities of the sample solutions were estimated by extrapolating both η_{sp}/c and $\ln\eta_r/c$ to zero concentration where η_{sp}/c and $\ln\eta_r/c$ were found to be linearly dependent on c. The addition of 0.02 wt.% NaN_3 produced no effect on the solution viscosities. The imogolite samples employed in a present study were characterized through Eq. (3). Assuming a rigid rod, the lengths of the imogolite samples were calculated from respective weight-average molecular weights as

$$L_w=8.4\times(M_w/4754)\ (\text{A}) \qquad (4)$$

where L_w denotes the weight-average rod length. The z-average mean-square radius of gyration is given in terms of m and L_w as

$$\langle S^2\rangle_z=\frac{(m+3)(m+2)}{(m+1)^2}\frac{L_w^2}{12} \qquad (5)$$

where m is a parameter to define a Schulz-Zimm type distribution for a rod length L:

$$W(L)=\frac{L^m}{\mathrm{m}!}y^{m+1}\exp(-yL) \qquad (6a)$$

$$y=(m+1)/L_w \qquad (6b)$$

The characteristics of the imogolite samples are summarized in Table 1 where the $\langle S^2\rangle_z$ values were calculated from Eqs. (4) and (5) with $m=5$ which is equivalent to $M_w/M_n=1.2$ as estimated previously.

Table 1. Characteristics of Imogolite Samples

Sample Code	$[\eta]$ (dl/g)	$M_w\times10^{-6}$	L_w(Å)	$\langle S^2\rangle_z^{1/2}$(Å)	L_w/d	$V\times10^{-5}$(Å^3)
Imogolite C-2	0.72	0.950*	1500	534*	59.2	7.48
Imogolite E	3.02	2.15	3800	1365	150.8	18.95
Imogolite F	1.58	1.55	2740	986	107.8	13.66

*) measured by light scattering.
V denotes the effective molecular volume calculated through the equation $V=\pi L_w d^2/4$.

The radius of gyration of the rod cross-section $\langle S_{cs}^2\rangle$ can be estimated from the Guinier plot for cross-section, since the scattered intensity I at angle θ follows an equation for the cross-sectional factor:[9]

$$I\cdot q=(I\cdot q)_0\exp(-\langle S_{cs}^2\rangle\cdot q^2/2) \qquad (7)$$

where q is the magnitude of a scattering vector at a scattering angle θ, given by:

$$q=(4\pi/\lambda)\sin(\theta/2) \qquad (8)$$

with λ being the wavelength of an incident beam.

The small-angle X-ray scattering (SAXS) measurements from imogolite solution were performed with a focusing optics SAXES (Small-Angle X-ray Equipment for Solutions) installed at the 2.5 GeV storage ring in Photon Factory of National Laboratory of High Energy Physics at Tsukuba.[10] The SAXS data were stored on 8" floppy disks through DEC MINC11/23 computer, and processed with FACOM M180II/AD at our Institute. The Guinier plot for cross-section is shown in Fig. 2 where Imogolite C-2 was used. See Table 1 for the C-2 characteristics. The radius of gyration of the cross-section was estimated from its slope to be 10.5 A. The initial slope in Fig. 2

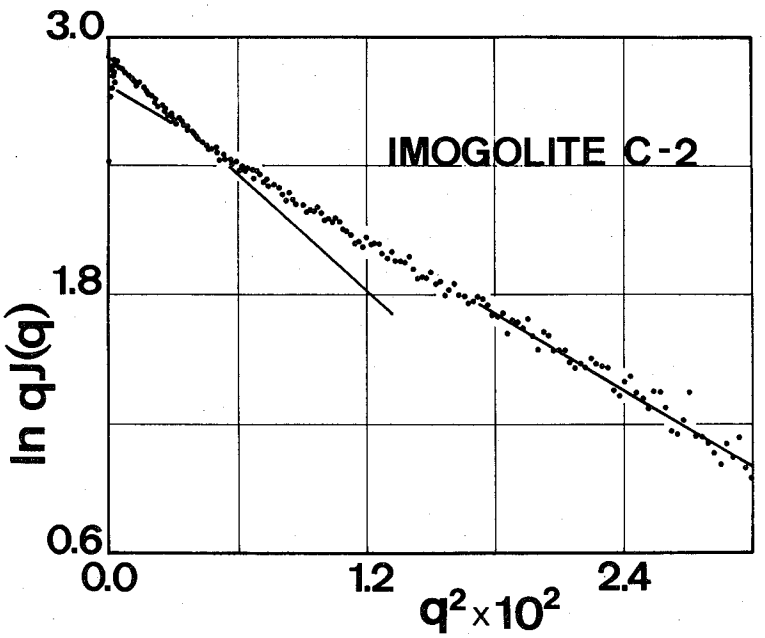

Fig. 2. Guinier plot for cross-section. (0.4 wt.% Imogolite C-2 in pH 3.0 acetic acid aqueous solution)

yields the radius of gyration of the cross-section as 13.8 A, suggesting a small amount of bimolecular aggregations observed as an second sedimentation peak in ultracentrifugation when the imogolite concentration exceeds 0.4 wt.%. Since the radius of gyration of a circular ring of radii r_a and r_i is calculated as

$$\langle S_{cs}^2\rangle=(r_a^2+r_i^2)/2, \qquad (9)$$

the diameter of imogolite is calculated to be 25.2 A (outer) and 15.5 A (inner) where $r_a/r_i\sim1.62$ was assumed from the electron microscopic observation (see Fig. 1). These values are somewhat larger than 23.0 A (outer) and 11.8 A (inner), respectively, estimated from the X-ray crystallographic data of dry imogolite films.[11] The difference is probably due to water molecules trapped in imogolite in solution. 25.2 A was used

as a cross-sectional diameter to calculate imogolite molecular volumes listed in Table 1. The imogolite molecular volume V in Table 1 denotes the effective volume responsible for a hard core repulsive interaction, and calculated through the equation:

$$V=\pi L_w d^2/4 \tag{10}$$

IMOGOLITE LIQUID CRYSTAL

When the imogolite concentration exceeds a certain limiting point (referred to as the A point), then the solution separates into two phases where the isotropic and anisotropic phases coexist. The entire solution becomes anisotropic above a higher imogolite concentration defined as the B point. The A point and B point were estimated by extrapolating the volume of the anisotropic phase (concentrated phase) and the volume of the isotropic phase (dilute phase) to zero, respectively. The phase diagram is shown in Fig. 3 for two imogolite samples. No temperature dependence was marked on the A and B points. Above the A point cholesteric spherulites were observed in the anisotropic phase through a polarization microscope (see Fig. 4). The cholesteric mesophase is characterized by the area of regular striations arranged in a swirl-like pattern. The striation separation S yields one-half the cholesteric pitch P_0 which was found to decrease with increasing imogolite concentrations as shown in Fig. 5. The cholesteric pitches were also determined from the laser diffraction pattern of imogolite solutions with a He-Ne laser. A satisfactory agreement was observed on the cholesteric pitches determined independently. Robinson[12] and DuPré[13] found an inverse dependence of the pitch on concentration with $P_0 \sim c^{-2.0}$ and $P_0 \sim c^{-1.8}$, respectively, in PBLG cholesteric liquid crystal solutions. Aqueous solutions of triple

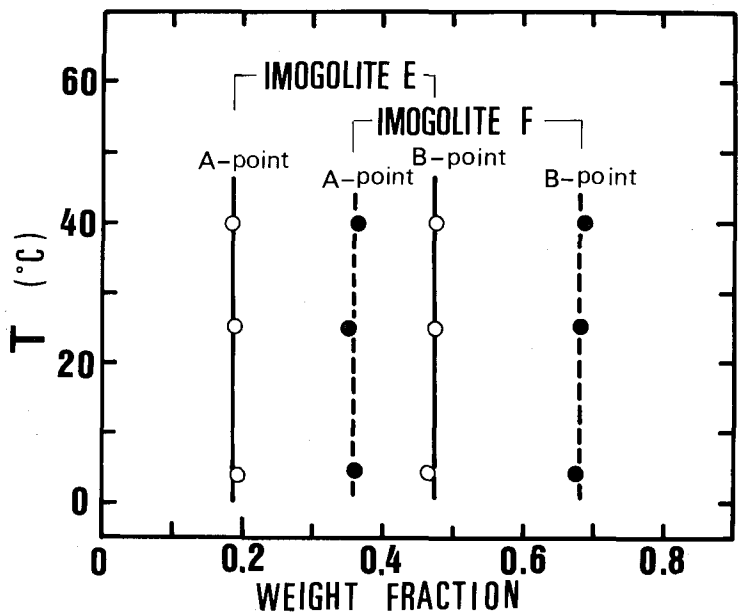

Fig. 3. T-v_2 phase diagram of imogolite. The biphasic regions correspond to the areas between A and B points as shown by arrows in the figure for Imogolite E and Imogolite F, respectively.

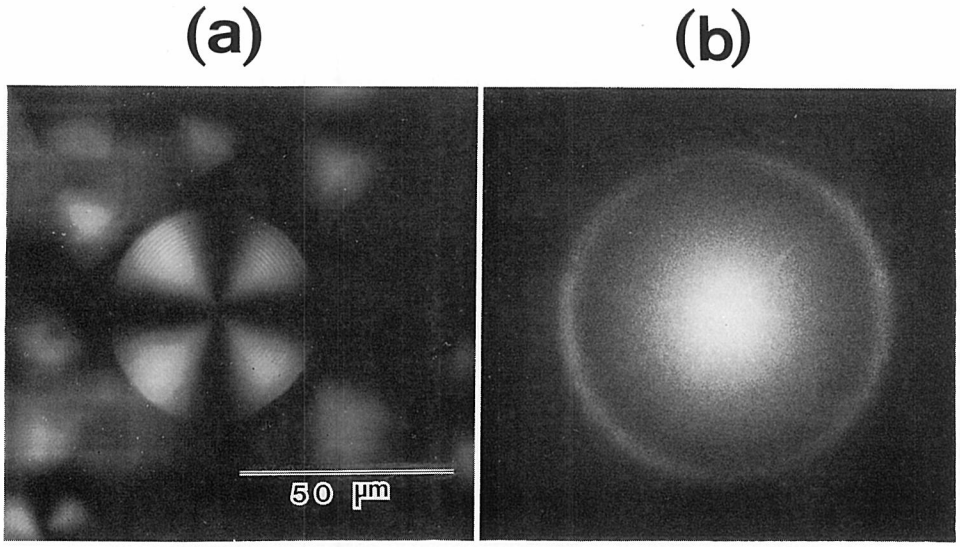

Fig. 4. (a) Cholesteric spherulites of imogolite and (b) the laser diffraction pattern from the cholesteric mesophase.

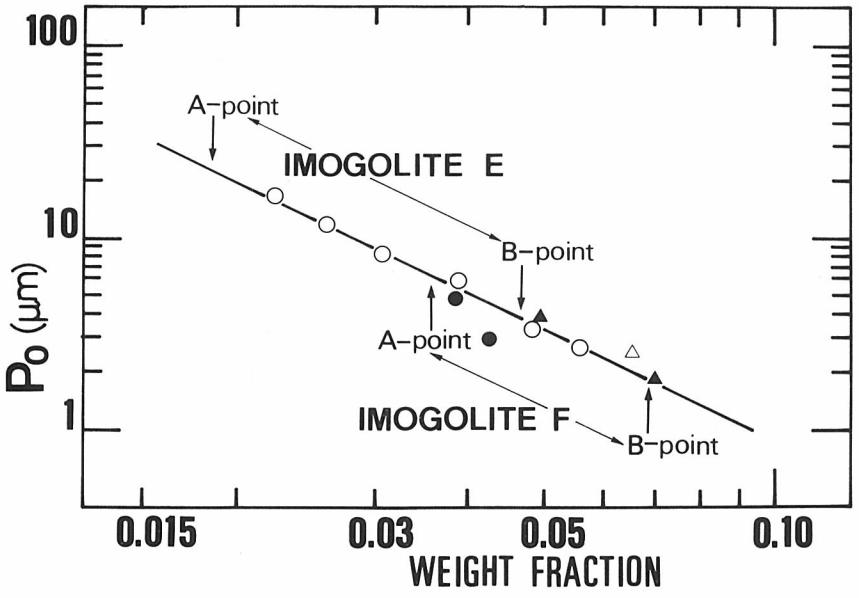

Fig. 5. Cholesteric pitch as a function of imogolite concentration. A points and B points are shown by arrows in the figure. White and black symbols denote Imogolite E and Imogolite F respectively where the circles and the triangles correspond to the cholesteric pitches estimated from the striation separation observed by a polarization microscope and by the laser diffraction respectively.

helical scleroglucan exhibit a similar concentration dependence of the cholesteric pitch ($P_0 \sim c^{-1.6}$) when the solute concentration exceeds the B point.[14] The concentration dependence is much milder in the biphasic region of scleroglucan solutions ($P_0 \sim c^{-0.4}$), and the transition with respect to the concentration dependence takes place at the

B point. The concentration dependence of the cholesteric pitch is approximated as $P_0 \sim c^{-1.9}$ above the A point of the imogolite solutions, and the molecular weight dependence was hardly observed on the cholesteric pitch in imogolite solutions, in contrast to the marked molecular weight dependence of the PBLG or scleroglucan cholesteric pitch.[13,14] No transition was observed at the B point of imogolite solutions. The A point and B point of imogolite solutions are much lower than those of PBLG or scleroglucan solutions, and Onsager's theory[3] shows a better quantitative agreement with the present results. Table 2 summarizes the critical volume fractions of Imogolites E and F expected from the theory of Flory or Onsager as well as those estimated from the phase diagram (Fig. 3). Here the experimental critical volume fractions were reduced in two ways from respective critical weight fractions evaluated directly from the phase diagram; i.e., (i) by a conventional manner using the specific volume of imogolite ($\bar{v}=0.327\ cm^3/g$) estimated previously,[7] or (ii) with the use of the effective molecular volumes calculated in Table 2. The volume fractions calculated

Table 2. Critical Volume Fraction

		Theory		Observed	
Imogolite		Onsager	Flory	(1)	(2)
E	v_2^*	0.0218	0.0523	0.0063	0.0101
	v_2^{**}	0.0280	0.0767	0.0158	0.0254
F	v_2^*	0.0305	0.0732	0.0117	0.0184
	v_2^{**}	0.0391	0.1073	0.0232	0.0364

Observed critical volume fractions (1) and (2) were reduced from corresponding critical weight fractions by the specific volume and the effective molecular volume, respectively.

in terms of the molecular volumes count the hollow parts as well in the effective volumes for a hard core repulsion, so that those are approximately 60% larger than the corresponding volume fractions reduced conventionally from the weight fractions with the imogolite specific volume. A quantitative agreement with Onsager's theory is satisfactory, especially with respect to the B points, when considered the effective volume of imogolite properly for a hard core repulsion. We found consistently smaller A point values than those expected from Onsager's theory, suggesting that the cholesteric ordering starts in lower concentrations and causes phase separation earlier than expected. The hard core repulsive interaction is a dominant factor to determine the B point, but there exists an intermolecular interaction to promote cholesteric ordering in the imogolite mesophase, which may also be responsible to shift the A point towards a lower concentration. This interaction is probably due to the positive charges on the outer surface of imogolite in acidic solutions, though the ordering mechanism of the imogolite mesophase is not yet known. An appreciable chain flexibility of PBLG or scleroglucan might have caused the shift of the A and B points towards higher concentrations. For example, a better quantitative agreement with Onsager's theory was observed in the aqueous solutions of schizophyllan triple helix when the axial ratio was small.[15] The A and B points of those solutions deviate from Onsager's

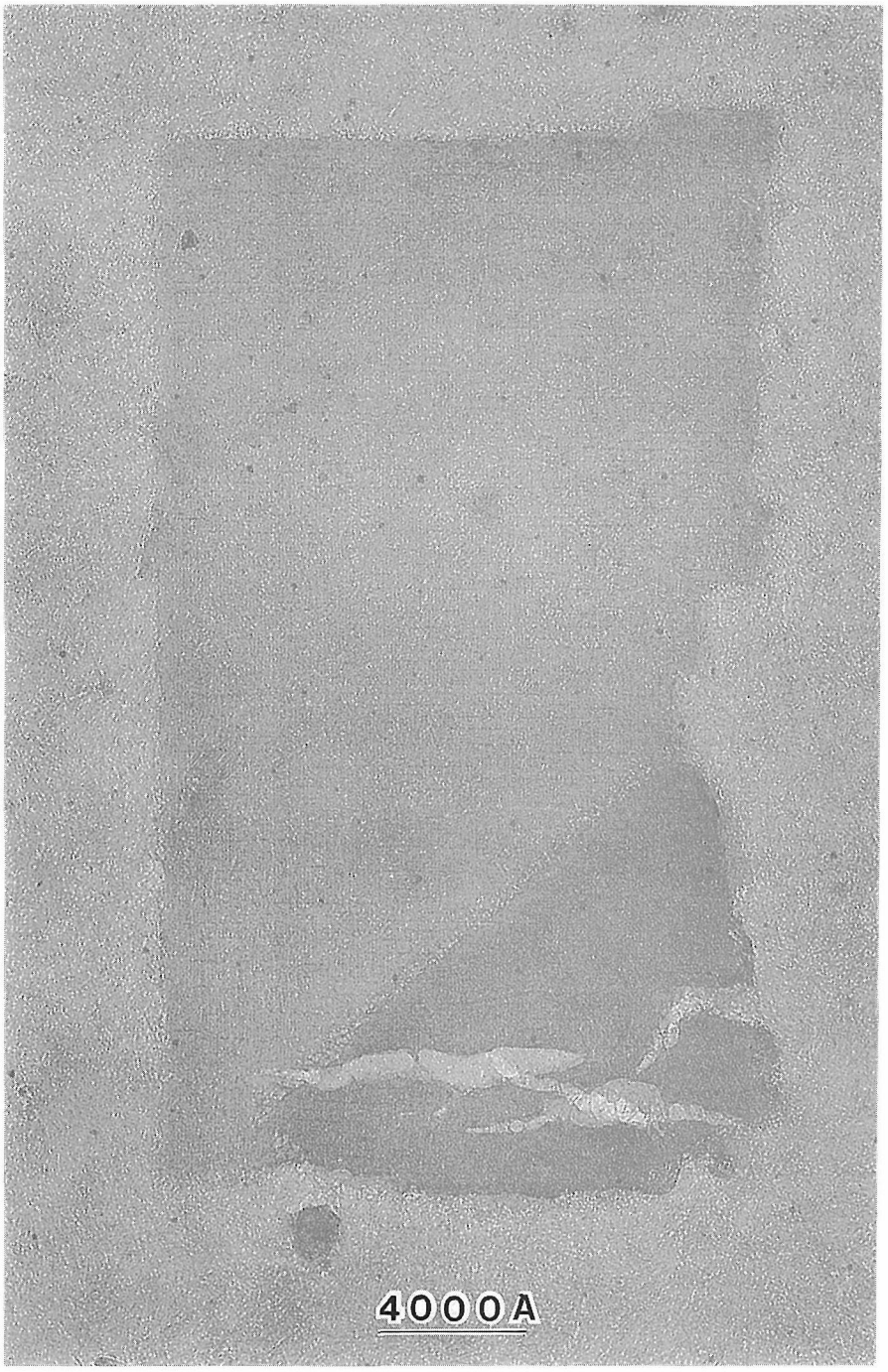

Fig. 6 (a).

Fig. 6. Raft-like imogolite sheet observed by electron microscope (Imogolite F). Scales are shown in the figure.

theory towards higher concentrations (predicted by Flory's theory) as the axial ratio increased. In his summary of the observed v_2^* values of PBLG and poly (*p*-benzamide) (PBA) *in various solvents in terms of Flory's theory, Ciferri has noted*[1] *the smaller* experimental values of v_2^* than expected by Eq. (1a) when the axial ratio was small. Thus, the agreement with Flory's theory[2] in the PBLG or PBA system[1] might be a mere artifact due to the semi-flexible nature of PBLG chain. It is generally agreed that the type of mesophase depends on the symmetry of the molecular interaction.

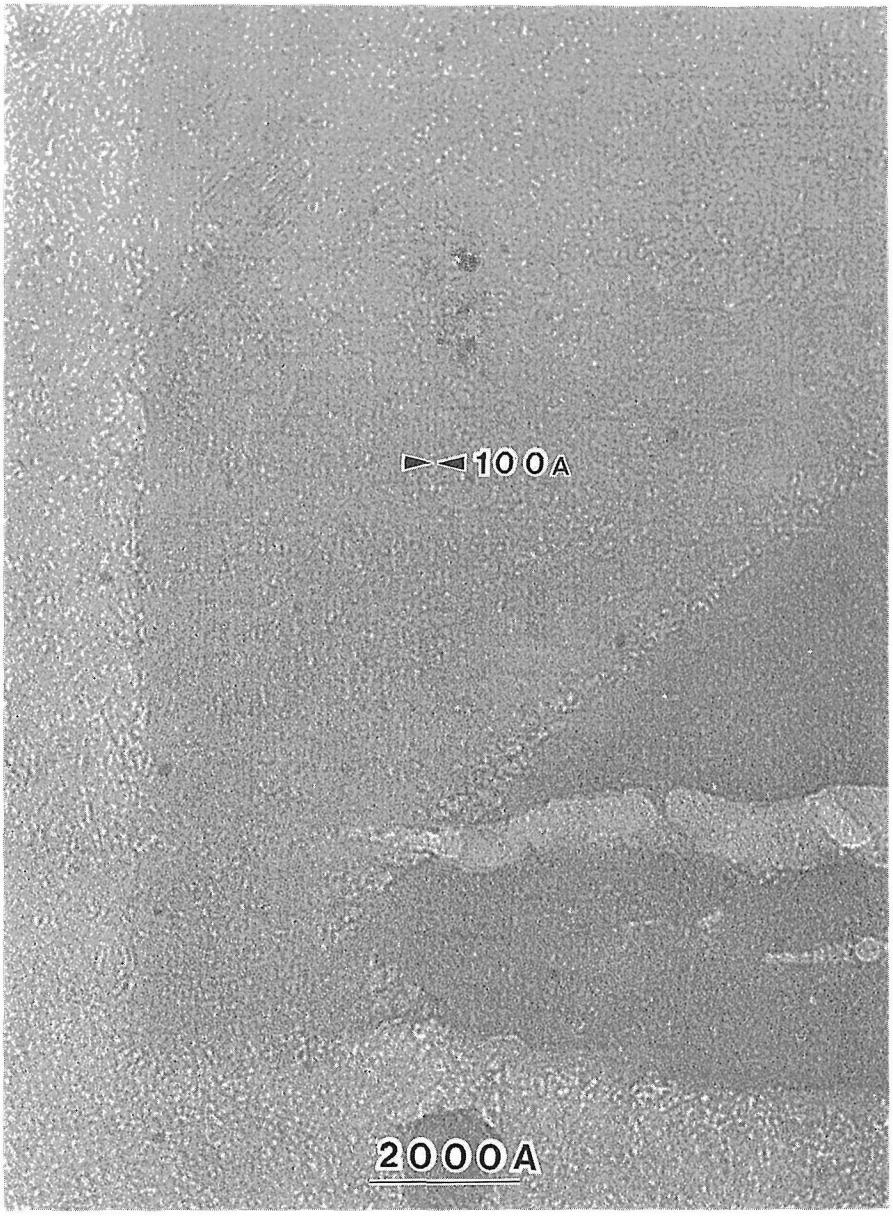

Fig. 6 (b).

That is, the chiral system represented by PBLG forms a cholesteric phase, but the achiral system such as PBA and imogolite should form nematic phases. The theories give account of the appearance of the cholesteric liquid crystalline ordering as due to the attractive dispersion potential inherent in the chiral molecules.[16,17] The cholesteric ordering is considered to reflect in some extent the twisted geometry of constituent molecules.[18] The imogolite mesophase contradicts this consensus, and is characterized by a cholesteric ordering as observed above. Though we do not know yet the origin of the twisting force to maintain the cholesteric ordering of the imogolite mesophase, an imogolite liquid crystal seems to consist of a pile of thin raft-like sheet twisted by a small angle. A raft-like imogolite sheet was in fact observed by an electron microscope which revealed imogolite molecules arranged parallel in sheet (see Fig. 6). Here a drop of the imogolite solution containing cholesteric mesophase (Imogolite F) was placed quietly on the carbon film of approximately 100 A thickness (treated in advance by glow-discharge to make hydrophilic), and stained with 1% uranyl acetate aqueous solution after eliminating excess fluid with a filter paper. Since imogolite is vulnerable to irradiation damage, the Minimum Dose System (MDS)[19] was employed to take its electron micrographs with JEOL-200CX Top Entry Type of accelerating voltage 200 kV (λ=0.025 A). Figure 6 was taken with a condition of 15 μm under focus in order to observe a periodic structure of 100 A in high contrast. The width of a raft unit is estimated to be 100 A equivalent to four imogolite cylinders, though it does not necessarily mean a raft-unit made of a unit of four imogolite cylinders arranged parallel. The periodic structure of imogolite sheet produced the striation pattern of 100 A interval and its boundary was distinguished electron-microscopically with some reason. Broken dark lines running vertically with respect to cylinder alignment were observed in parts in Fig. 6. Those dark lines are caused by uranyl acetate stain trapped probably in the gaps between two jointed groups of aligned imogolite ends. A group of imogolite ends seem to be aligned and form a line as demonstrated by the broken dark lines and sharp edges of the raft-like imogolite sheet. That is, a raft-like sheet seems to be composed of bunches of imogolite cylinders standing side by side to align their ends in a row. The distances between a set of two broken lines are 2500–2900 A which corresponds approximately to the rod length of Imogolite F. At high magnification, a single imogolite cylinder is seen and its diameter was estimated to be 24–25 A in good agreement with 25.2 A estimated by SAXS (see Fig. 1). A full structural analysis of a raft-like sheet will be expected in a forthcoming report.

CONCLUDING REMARKS

The mesophase of imogolite solutions is characterized with low A and B points in comparison with the mesophase of quasi-rigid chains such as PBLG and scleroglucan. Onsager's theory exhibits a better quantitative agreement with our results when taken into account the effective volume of imogolite properly for a hard core repulsion. A cholesteric ordering starts in lower concentrations than Onsager predicted. The ordering is localized and raft-like imogolite sheet floating in the solution were observed by an electron microscope. Considering imogolite charged positive in acidic solutions, this ordering phenomenon is probably due to the similar ordering mechanism of charged

latex particles or macroions in dilute solutions.[20] Imogolite is achiral, yet its liquid crystalline ordering seems cholesteric against the expectation of available theories.[1]

ACKNOWLEDGEMENT

We are indebted to Dr. M. Nagura, Shinshu University, for his experimental help at Photon Factory. Thanks are due to Dr. M. Tsuji for his participation in some part of the experiment .

REFERENCES

(1) See for example, *Polymer Liquid Crystals*, (ed. by A. Ciferri, W. R. Krigbaum and R. B. Meyer), Academic Press, New York, 1982.
(2) P. J. Flory, *Proc. R. Soc. (London)*, **A234**, 73 (1956); P. J. Flory and G. Ronca, *Mol. Cryst. Liq. Cryst.*, **54**, 289 (1976).
(3) L. Onsager, *Ann. N.Y. Acad. Sci.*, **51**, 627 (1949); R. F. Kayser Jr. and H. J. Raveche, *Phys. Rev.*, **A17**, 2067 (1978).
(4) W. G. Miller, Jr., J. H. Rai and E. L. Wee, In *Liquid Crystals and Ordered Fluids*, (ed. by J. F. Johnson and R. S. Porter), Vol. 2, P243, Plenum, New York, 1976.
(5) P. Navard, J. M. Haudin, S. Dayan and P. Sixou, *J. Polymer Sci. Polym. Lett.*, **19**, 379 (1981).
(6) M. Warner and P. J. Flory, *J. Chem. Phys.*, **73**, 6327 (1980).
(7) N. Donkai, H. Inagaki, K. Kajiwara, H. Urakawa and M. Schmidt, *Makromol. Chem.*, in press.
(8) Y. Horikawa, *Clay Sci.*, **4**, 255 (1975).
(9) G. Porod, *Z. Naturforsch.*, **4a**, 401 (1949).
(10) T. Ueki, Y. Izumi, H. Tagawa, Y. Hiragi, M. Kataoka, Y. Muroga, T. Matsushita and Y. Amemiya, *KEK Internal*, to appear.
(11) P. D. G. Cradwick, V. C. Farmer, J. D. Russel, C. R. Masson, K. Wada and N. Toshinaga, *Nature Phys. Sci.*, **240**, 187 (1972).
(12) C. Robinson, J. C. Ward and R. B. Beevers, *Disc. Faraday Soc.*, **25**, 29 (1958); C. Robinson, *Tetrahedron*, **13**, 219 (1961).
(13) D. B. DuPré and R. W. Duke, *J. Chem. Phys.*, **63**, 143 (1975).
(14) T. Yanaki, T. Norisuye and A. Teramoto, *Polmer J.*, **16**, 165 (1984).
(15) K. Van, *Ph. D. Thesis*, Osaka University, 1984.
(16) W. J. A. Goossens, *Mol. Cryst. Liq. Cryst.*, **12**, 237 (1971).
(17) H. Kimura, M. Hosino and H. Nakano, *J. Phys. Soc. Japan*, **51**, 1584 (1982).
(18) J. P. Straley, *Phys. Rev.*, **A14**, 1835 (1976).
(19) Y. Fujiyoshi, T. Kobayashi, K. Ishizuka, N. Uyeda, Y. Ishida and Y. Hamada, *Ultramicroscopy*, **5**, 459 (1980).
(20) N. Ise, *Makromol. Chem. Suppl.*, **12**, 215 (1985).